Chemical Engineering Science 84 (2012) 564–573

Contents lists available at SciVerse ScienceDirect

Chemical Engineering Science

journal homepage: www.elsevier.com/locate/ces

Energy and exergy analyses of a Cu–Cl cycle based integrated system for hydrogen production

T.A.H. Ratlamwala *, I. Dincer

Faculty of Engineering and Applied Science, University of Ontario Institute of Technology, 2000 Simcoe Street North, Oshawa, Ontario, Canada L1H 7K4

HIGHLIGHTS

- Study of a Cu–Cl cycle based integrated system for hydrogen production.
- Thermodynamic analysis of the system through energy and exergy.
- Effect of operating parameters on the performance of the system.

ARTICLE INFO

Article history:
Received 29 May 2012
Received in revised form
24 August 2012
Accepted 27 August 2012
Available online 7 September 2012

Keywords:
Cu–Cl thermochemical cycle
Kalina cycle
Hydrogen production
Energy
Exergy
Efficiency

ABSTRACT

This paper analyzes an integrated Cu–Cl thermochemical cycle, Kalina cycle and electrolyzer for hydrogen production. The system operating parameters such as mass fraction, pressure and temperature are varied to investigate their effects on the energy and exergy efficiencies of the with/without heat recovery and integrated system, rate of hydrogen production, and rate of oxygen production. A new Cu–Cl design layout is then presented with a heat exchanger network developed to recover heat within the Cu–Cl cycle in the most efficient manner. The exergy destruction rate in each component is determined and discussed. The results show that increasing the electrolyzer temperature is beneficial up to 328.6 K, after which the performance of the cycle results in a negative trend. The exergy efficiency varies more significantly with operating parameters than the corresponding energy efficiency. The maximum exergy destruction in the Cu–Cl cycle occurs in the first separator (16.82 kW) and in the heat exchanger of the Kalina cycle (48.05 kW), so these components should be considered for performance improvement of the system.

1. Introduction

Energy plays a vital role in our daily life as it is required to operate almost all systems and applications around us. At present, fossil fuels act as a the main source which emits harmful greenhouse gases, such as CO_2, NO_x, etc. and are responsible for environmental damages.

The increased emissions of greenhouse gases and depletion of ozone layer have forced researchers around the globe to come together with a solution to the fossil fuel technologies. Thus, they have responded to this challenge by developing hydrogen as an energy carrier. Studies conducted by researchers (Turner, 2004; Moriarty and Honnery, 2009) show that hydrogen is a great contender for becoming a leading energy carrier in the future for environmental benign and sustainable development. The major benefit of hydrogen as compared to fossil fuel is that systems utilizing hydrogen as an energy carrier do not emit harmful greenhouse gases. It is expected that in future the role of hydrogen will become prominent as the world's shift from an era of fossil fuels to an era of cleaner fuels (Turner, 2004; Moriarty and Honnery, 2009; Muradov and Veziroglu, 2008; Midilli and Dincer, 2009, 2008).

Although, hydrogen can be looked at as an environmentally-benign energy carrier but it is not freely available in the atmosphere. There are several ways of producing the hydrogen which include (a) the steam methane reforming (SMR), (b) the water electrolysis, (c) the coal gasification and (d) the thermochemical cycles. Dufour et al. (2009) stated that at present 96% of the hydrogen is produced using the SMR. The SMR has a disadvantage of releasing CO_2, while electrolyzers consume high electrical power in order to produce hydrogen through dissociation of water molecules. Giaconia et al. (2011) outlined that thermochemical water-splitting cycles (TWSCs) represent an appealing carbon-free option for hydrogen production powered by alternative (carbon-free) energy sources. A thermochemical cycle is a process consisting of a closed loop of thermally driven chemical reactions, where water is decomposed into hydrogen and oxygen, and all other intermediate compounds are recycled (Aghahosseini et al., 2011). Many TWSCs have been studied and evaluated, but very few of

* Corresponding author. Tel.: +1 647 785 1765.
E-mail addresses: tahir.ratlamwala@uoit.ca (T.A.H. Ratlamwala), ibrahim.dincer@uoit.ca (I. Dincer).

0009-2509/$ - see front matter © 2012 Elsevier Ltd. All rights reserved.
http://dx.doi.org/10.1016/j.ces.2012.08.052

these technologies have made it to the level of elaborative research and pilot plants (Ozbilen et al., 2011). At present, some major hindrances to vast scale of hydrogen production using TWSCs are high temperature requirements and high production cost of these cycles. Out of many thermochemical cycles present in the literature, the Cu–Cl cycle holds an edge in terms of temperature requirement and handling. Several researchers (Naterer et al., 2011a, 2011b; Ferrandon et al., 2010) stated that due to the lower operating temperature requirements of the Cu–Cl cycle (around 530 °C), it has reduced material and maintenance costs as compared to other thermochemical cycles.The major benefit of Cu–Cl cycle is that it offers one of the highest efficiencies among all TWSCs and requires lower operating temperatures. Studies conducted by several researchers (Orhan et al., 2011; Lewis et al., 2010; Zamfirescu et al., 2010) have shown that Cu–Cl cycle efficiencies can reach up to 55%, based on the operating and design conditions.

The Cu–Cl cycles may be divided into three categories namely three step, four step and five step Cu–Cl cycle. The difference among these steps is the number of processes required to produce hydrogen. The system′s energy requirements, efficiency and environmental impact are highly dependent on the number of steps. Efficiency comparative study conducted by Orhan et al. (2012) found that the four step Cu–Cl cycle has lower energy consumption rate and best efficiency among all three steps. Another comparative study conducted by Ozbilen et al. (2011) mentioned that from environmental perspectives the four step Cu–Cl cycle performed best as it has impacts on the environment in the least possible manner.

In this paper, we study an integrated Cu–Cl thermochemical cycle and Kalina cycle system for hydrogen production. An integrated system recovers waste heat in order to produce addition output which can benefit both the environment and the plant's operating firm. A new design of the four step Cu–Cl cycle is developed and studied. The heat exchangers network is developed for better heat recovery within the system. The waste heat released by the Cu–Cl cycle is recovered and is used to produce power using a Kalina cycle and this power is supplied to electrolyzer for external hydrogen production. A parametric study is conducted to investigate the effect of several operating parameters such as mass fraction of hydrochloric acid, electrolyzer pressure, electrolyzer temperature and ambient temperature on the rate of hydrogen produced, rate of oxygen produced and energy and exergy efficiencies of the system. A comparative study is also carried out to see the effect of operating parameters on the efficiencies of three Cu–Cl cycle cases namely system without heat recovery, system with heat recovery and integrated system. In the end, an exergy destruction bar chart is presented for a base case to show which component in the cycle destructs the most amount of exergy.

2. System description

Several set of reactions are conducted in the Cu–Cl cycle to achieve the overall splitting of water into hydrogen and oxygen. The overall net reaction is $2H_2O\,(l) \rightarrow 2H_2\,(g) + O_2\,(g)$. The chemical reactions taking place in Cu–Cl cycle form a closed internal loop that recycles all chemicals on a continuous basis, without emitting any greenhouse gases.

2.1. Four step Cu–Cl cycle

The four step Cu–Cl cycle studied in this paper is shown in Fig. 1. The four step Cu–Cl cycle is divided into the following four steps: (a) hydrolysis, (b) oxygen production, (c) hydrogen production and (d) drying.

In hydrolysis section high temperature steam at approximately 400 °C is brought in contact with solid $CuCl_2$. The reaction takes place and the products coming out of hydrolysis section are

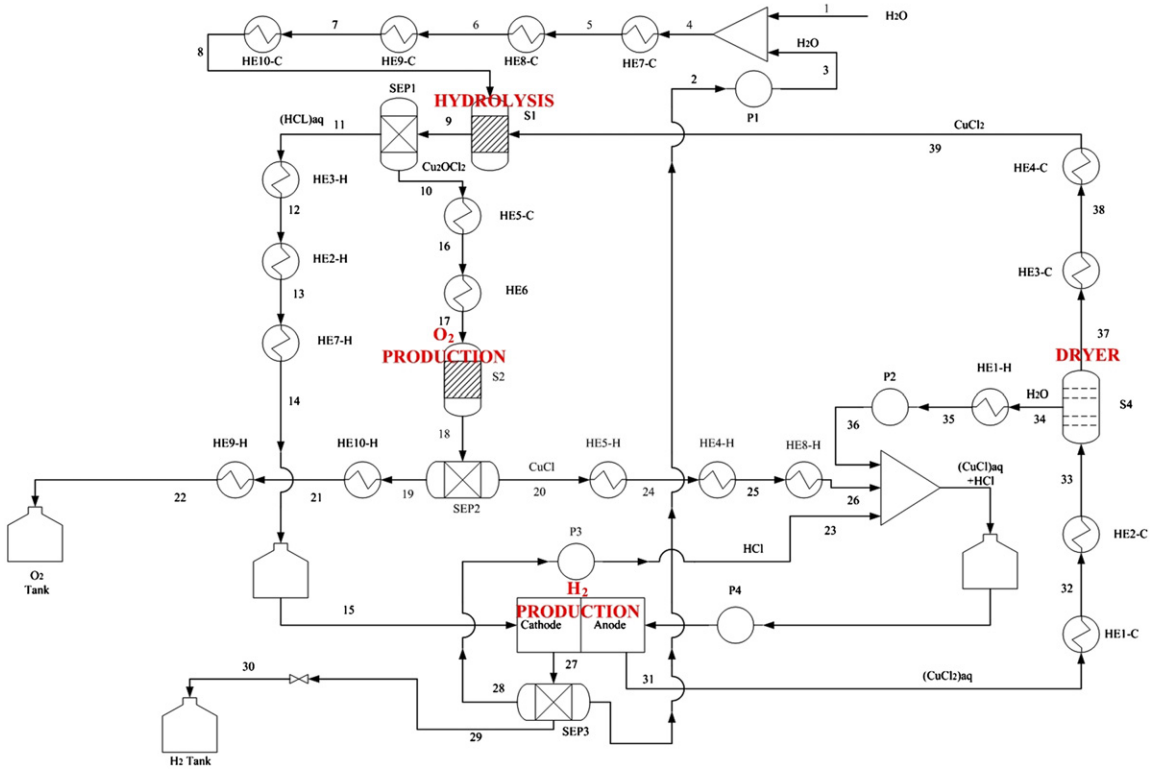

Fig. 1. Schematic diagram of four step Cu–Cl cycle (second option).

aqueous HCL and solid Cu_2OCl_2. The overall reaction is presented below

$$2CuCl_2\,(s)+H_2O\,(g)\rightarrow Cu_2OCl_2\,(s)+2HCl\,(g)$$

The second reaction which takes place in four step Cu–Cl cycle is oxygen production. This is the most energy consuming step of the cycle as in this step temperature required for oxygen production is approximately 500 °C. Cu_2OCl_2 is passed through two heat exchangers before it reaches a second separator denoted by SEP2 in Fig. 1. In this separator Cu_2OCl_2 is broken in to CuCl and oxygen. The gaseous oxygen produced is passed through several heat exchangers where its temperature is brought down in order to make it available for later use. The CuCl produced is passed through several heat exchangers where its temperature is brought down in order to supply it to the mixture where it is mixed with water and HCl. The separation reaction which takes place in this step is as follows:

$$Cu_2OCl_2\,(s)\rightarrow +2CuCl\,(1)+1/2O_2\,(g)$$

The third step in four step Cu–Cl cycle is the hydrogen production step. This step takes place at a temperature lower than 100 °C. In this step aqueous CuCl and HCl from the mixture enter the electrolyzer. In the electrolyzer electrical energy is provided to dissociate CuCl and HCl into aqueous $CuCl_2$ and H_2. The hydrogen produced is sent to the storage tank whereas aqueous $CuCl_2$ produced is passed through the heat exchanger network where its temperature is increased in order to separate water from the solution. The reaction that takes place in this step is presented as follows:

$$2CuCl_2(aq)+2HCl(aq)\rightarrow CuCl_2(aq)+H_2(g)$$

The final step in four step Cu–Cl cycle is drying. In the drying process water is removed from the aqueous $CuCl_2$. The dried $CuCl_2$ in solid form is then passed through the heat exchangers to enter the hydrolysis section. The water separated from the aqueous $CuCl_2$ is pumped to the pressure of the mixture and is passed through the heat exchanger in order to bring down its temperature to that of the mixture.

Most of the heat requirement of the four step Cu–Cl cycle is met by recycling the waste heat within the cycle. For the heat recycling purpose a heat exchanger network is developed as shown in Fig. 2. This heat exchanger network recovers maximum amount of heat within the cycle in order to reduce the energy demand of the cycle and enhance its efficiency. The water at 851.2 K is supplied to the heat exchanger network in order to match the temperature requirement of the Cu–Cl cycle which requires temperature as high as 773 K.

2.2. Kalina cycle

The water stream coming out of the heat exchanger network of Cu–Cl cycle is at approximately 373 K and can be further used for power generation using the Kalina cycle. In the Kalina cycle heat is supplied to the generator as shown in Fig. 2. In the generator strong solution of ammonia–water enters at state k3 which is then heated-up to leave at higher temperature at state k4. The strong solution of ammonia–water leaving at state k4 then enters the separator where ammonia–water vapor is removed at state k8 and the weak ammonia–water solution is removed at state k5. The ammonia–water vapor is then expanded in the turbine and power is produced. The expanded ammonia–water leaves the turbine at state k9 to enter condenser where its temperature is brought down before it enters the absorber at state k10. The weak solution leaving the separator passes through the heat exchanger where it releases heat to the incoming strong solution at state k2. After releasing heat in the heat exchanger, the weak solution passes through the expansion valve where its pressure is brought down to that of the absorber. In the absorber, weak solution at state k7 and ammonia–water vapor at state k10 mix together to leave at state k1 as strong solution in liquid form.

2.3. Heat recovery system

A heat exchanger network is developed to recover the maximum amount of heat from the Cu–Cl cycle considered here. In

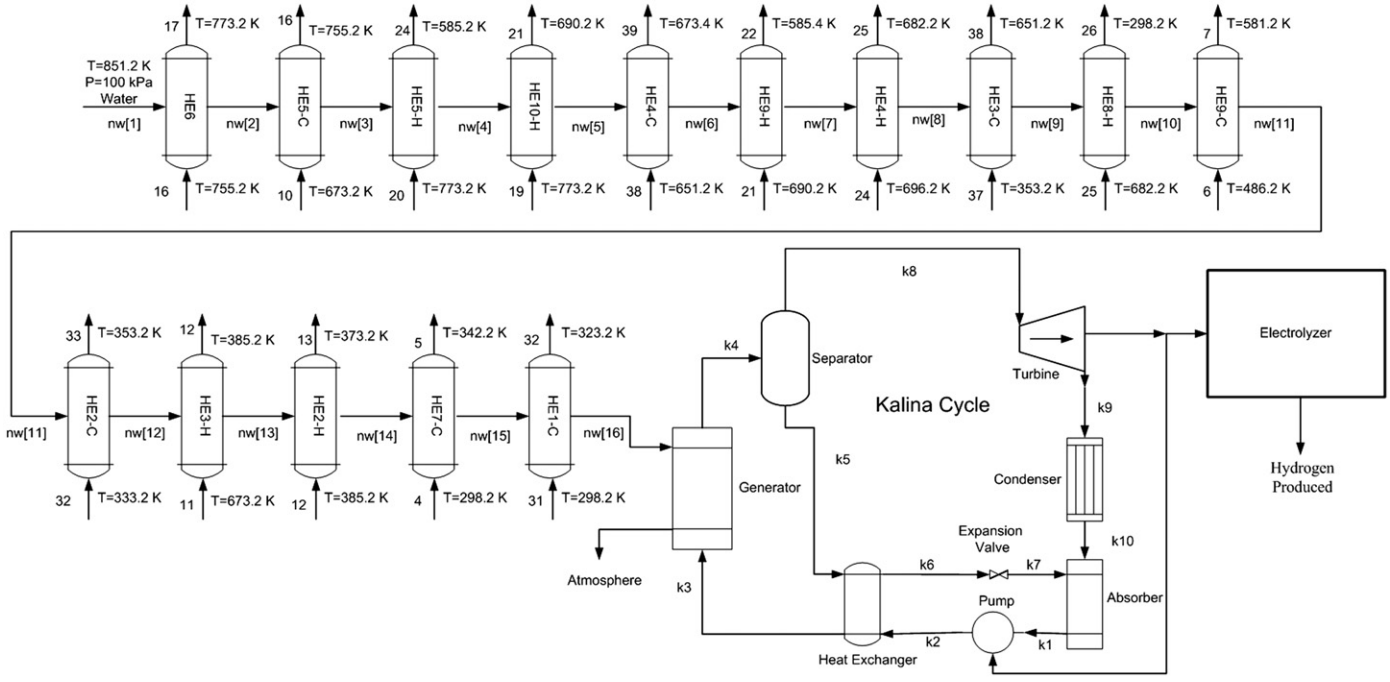

Fig. 2. Schematic diagram of heat exchanger network and the Kalina cycle.

this network a hot water from energy source at state *nw*[1] is supplied to the HE6 in order to heat the fluid running through it from 755.2 K to 773.2 K in order to meet the high temperature requirement of the cycle. The hot water then enters the HE5-C at state *nw*[2] where it releases heat to raise the temperature of the fluid from 673.2 K to 755.2 K. Then the hot water at state *nw*[3] enters the HE5-H where it gains heat from the fluid running in the heat exchanger and helps bringing down its temperature from 773.2 K to 585.2 K. The heated water at state *nw*[4] then enters the HE10-H where it gains heat from the flowing solution in order to cool it down from 773.2 K to 690.2 K. The hot water at state *nw*[5] then enters the HE4-C where it releases heat to raise the temperature of flowing solution from 651.2 K to 673.4 K. The relatively cooler water then enters the HE9-H at state *nw*[6], where it gains heat from the flowing solution to cool it down from 690.2 K to 585.4 K. After gaining heat in the HE9-H the hot water at state *nw*[7] enters HE4-H to gain heat from the flowing solution in order to drop its temperature from 696.2 K to 682.2 K. The hot water then enters the HE3-C at state *nw*[8], where it releases heat to raise the temperature of flowing solution from 353.2 K to 651.2 K. The relatively cooled water then enters the HE8-H at state *nw*[9] in order to gain heat from the solution flowing through it to drop its temperature from 682.2 K to 298.2 K. The hot water then enters the HE9-C at state *nw*[10] and releases heat to raise the temperature of flowing solution from 486.2 K to 581.2 K. After releasing heat the water at state *nw*[11] enters HE2-C where it is used to raise the temperature of the flowing solution from 333.2 K to 353.2 K. After releasing heat, the water enters the HE3-H at state *nw*[12] in order to bring down to the temperature of flowing solution from 673.2 K to 385.2 K. The relatively hot water then enters the HE2-H at state *nw*[12] so that the temperature of the flowing solution can be brought down from 385.2 K to 373.2 K. After gaining heat, the water at state *nw*[14] enters the HE7-C to release heat to the flowing solution to raise its temperature from 298.2 K to 342.2 K. After releasing heat, the water at state *nw*[15] enters the HE1-C in order to release heat to the flowing solution to raise its temperature from 298.2 K to 323.2 K. The water leaving the HE1-C at state *nw*[16] enters the generator of Kalina cycle, where it releases heat to ammonia–water mixture before leaving the generator at atmospheric temperature. The high temperature of requirement of Cu–Cl cycle can be fulfilled either by waster nuclear heat or solar thermal source through e.g., heliostat field.

2.4. Energy and exergy analyses

The following assumptions will be adopted in the analysis. The ambient conditions are 298.15 K and 101 kPa. The system is operating at steady state. The heat exchanger effectiveness is assumed to be 100%, while the pump and turbine isentropic efficiencies are taken as 80% based on the study conducted by Dincer and Rosen (2007). The Kalina cycle pressures are taken as 250 kPa and 400 kPa. The concentrations (mass basis) of strong solution, weak solution, and ammonia–water vapor are taken as 0.6 kg/kg, 0.4 kg/kg and 0.9 kg/kg, respectively. The parasitic losses are assumed to be about 20%. The energy conversion ratio from heat to power is taken as 0.4.

General energy and exergy balance equations of the integrated system are presented in this section. The specific enthalpy at any given state in the Cu–Cl cycle is calculated as

$$h_i = \sum_{m=1}^{k} mf_m h_m \tag{1}$$

The specific entropy at any given state in the Cu–Cl cycle is calculated as

$$s_i = \sum_{m=1}^{k} mf_m s_m \tag{2}$$

The mass fraction of a substance is found by

$$mf_m = y_m \frac{M_m}{M_i} \tag{3}$$

where

$$M_i = \sum_{m=1}^{k} y_m M_m$$

The exergy rate at any given state in the Cu–Cl cycle is

$$\dot{E}x_i = \dot{m}_i((h_i - h_0) - T_0(s_i - s_0)) \tag{4}$$

The thermal exergy rate in each heat exchanger is defined as

$$\dot{E}x_{th_i} = \left(1 - \frac{T_0}{T_i}\right)\dot{Q}_i \tag{5}$$

The power required by any pump in Cu–Cl cycle is written as

$$\dot{W}_{p_i} = \dot{m}_i(h_i - h_{i-1}) \tag{6}$$

The heat supplied to the generator of the Kalina cycle is defined as

$$\dot{Q}_g = \dot{m}_{nw}(h_{nw[16]} - h_{nw[0]}) \tag{7}$$

The power that can be obtained from the turbines of a Kalina cycle is calculated as follows:

$$\dot{W}_{turb} = \dot{m}_{k8}(h_{k8} - h_{k9}) \tag{8}$$

The power consumed by the pump in the Kalina cycle is given by

$$\dot{W}_{p_k} = \dot{m}_{k1}(h_{k2} - h_{k1}) \tag{9}$$

In the model, parasitic losses are also considered. The percentage of parasitic losses is assumed to be 20%. The parasitic losses are defined as

$$\dot{W}_{parasitic} = 0.2(\dot{W}_{turb} - \dot{W}_{p_k}) \tag{10}$$

The actual net power output that can be obtained from the Kalina cycle is

$$\dot{W}_{net_k} = \dot{W}_{turb} - \dot{W}_{p_k} - \dot{W}_{parasitic} \tag{11}$$

The power produced by the Kalina cycle is supplied to the electrolyzer for additional hydrogen production. The electrolyzer considered in this study is the one readily available in the market which uses electricity to dissociate water molecule. The amount of hydrogen produced by the electrolyzer is

$$\dot{m}_{H_{2,ext}} = \frac{\eta_{elec}\dot{W}_{net_k}}{HHV} \tag{12}$$

where $\eta_{elec} = 56\%$. The exergetic content of hydrogen is obtained by

$$\dot{E}X_{H_2} = \dot{m}_{H_2}[ex_{H_2,ch} + ex_{H_2,ph}] \tag{13}$$

where

$$ex_{H_2,ch} = \frac{235.153 \times 1000}{M_{H_2}}$$

$$ex_{H_2,ph} = \left[(h_{H_2} - h_0) - T_0(s_{H_2} - s_0)\right]$$

Note that the exergy content of hydrogen is 235.15 kJ/g mol according to Dincer and Rosen (2007).

The energy and exergy efficiencies of the Cu–Cl cycle without heat recovery are defined as

$$\eta_{en_{wohr}} = \left(\frac{\dot{m}_{29}\, HHV_{H_2} + \dot{m}_{22} h_{22}}{\dot{Q}_{HE1\text{-}C} + \dot{Q}_{HE2\text{-}C} + \dot{Q}_{HE3\text{-}C} + \dot{Q}_{HE4\text{-}C} + \dot{Q}_{HE5\text{-}C} + \dot{Q}_{HE7\text{-}C} + \dot{Q}_{HE8\text{-}C} + \dot{Q}_{HE9\text{-}C} + \dot{Q}_{HE10\text{-}C} + \dot{Q}_{HE6} + \dot{Q}_{S1} + \dot{Q}_{S2} + \dot{Q}_{S4} + \dot{m}_1 h_1 + \frac{(\dot{W}_{elec} + \dot{W}_{p1} + \dot{W}_{p2} + \dot{W}_{p3} + \dot{W}_{p4})}{\eta_{conv}}} \right) \tag{14}$$

$$\eta ex_{wohr} = \left(\frac{\dot{E}x_{H2} + \dot{E}x_{32}}{\dot{E}x_{HE1\text{-}C} + \dot{E}x_{HE2\text{-}C} + \dot{E}x_{HE3\text{-}C} + \dot{E}x_{HE4\text{-}C} + \dot{E}x_{HE5\text{-}C} + \dot{E}x_{HE7\text{-}C} + \dot{E}x_{HE8\text{-}C} + \dot{E}x_{HE9\text{-}C} + \dot{E}x_{HE10\text{-}C} \dot{E}x_{HE6} + \dot{E}x_{s1} + \dot{E}x_{s2} + \dot{E}x_{s4} + \dot{E}x_1 + \frac{(\dot{W}_{elec} + \dot{W}_{p1} + \dot{W}_{p2} + \dot{W}_{p3} + \dot{W}_{p4})}{\eta_{conv}}} \right) \tag{15}$$

The energy and exergy efficiencies of the Cu–Cl cycle with heat recovery are given by

$$\eta_{en_{whr}} = \left(\frac{\dot{m}_{29}\, HHV_{H_2} + \dot{m}_{22} h_{22}}{\dot{Q}_{HE8\text{-}C} + \dot{Q}_{HE10\text{-}C} + \dot{Q}_{S1} + \dot{Q}_{S2} + \dot{Q}_{S4} + \dot{m}_1 h_1 + \dot{m}_{nw}(h_{nw[1]} - h_{nw[16]}) + \frac{(\dot{W}_{elec} + \dot{W}_{p1} + \dot{W}_{p2} + \dot{W}_{p3} + \dot{W}_{p4})}{\eta_{conv}}} \right) \tag{16}$$

$$\eta_{ex_{whr}} = \left(\frac{\dot{E}x_{H_2} + \dot{E}x_{32}}{\dot{E}x_{HE8\text{-}C} + \dot{E}x_{HE10\text{-}C} + \dot{E}x_{S1} + \dot{E}x_{S2} + \dot{E}x_{S4} + \dot{E}x_1 + \dot{E}x_{nw[1]} - \dot{E}x_{nw[16]} + \frac{(\dot{W}_{elec} + \dot{W}_{p1} + \dot{W}_{p2} + \dot{W}_{p3} + \dot{W}_{p4})}{\eta_{conv}}} \right) \tag{17}$$

The energy and exergy efficiencies of the integrated system are defined as

$$\eta_{en_{wi}} = \left(\frac{\dot{m}_{29}\, HHV_{H_2} + \dot{m}_{22} h_{22} + (\dot{m}_{H_2}\, HHV_{H_2})_{elec}}{\dot{Q}_{HE8\text{-}C} + \dot{Q}_{HE10\text{-}C} + \dot{Q}_{S1} + \dot{Q}_{S2} + \dot{Q}_{S4} + \dot{m}_1 h_1 + \dot{m}_{nw}(h_{nw[1]} - h_{nw[0]}) + \frac{(\dot{W}_{elec} + \dot{W}_{p1} + \dot{W}_{p2} + \dot{W}_{p3} + \dot{W}_{p4})}{\eta_{conv}}} \right) \tag{18}$$

and

$$\eta_{ex_{wi}} = \left(\frac{\dot{E}x_{H_2} + \dot{E}x_{32} + \dot{E}x_{H_{2,elec}}}{\dot{E}x_{HE8\text{-}C} + \dot{E}x_{HE10\text{-}C} + \dot{E}x_{S1} + \dot{E}x_{S2} + \dot{E}x_{S4} + \dot{E}x_1 + \dot{E}x_{nw[1]} + \frac{(\dot{W}_{elec} + \dot{W}_{p1} + \dot{W}_{p2} + \dot{W}_{p3} + \dot{W}_{p4})}{\eta_{conv}}} \right) \tag{19}$$

In order to solve the above equations, Klein (2012) is used to obtain thermophysical properties of the working fluids and then solve the mass, energy and exergy balance equations.

3. Results and discussion

Predictions of the integrated system performance are presented in this section. The predictions of the Cu–Cl cycle are validated by comparing results with the data provided by Lewis et al. (2010). The predicted efficiency in this study is found to be 52% as compared to 55% reported by Lewis et al. (2010). The Kalina cycle is validated by comparing results with data presented by Bombarda et al. (2012). The predicted efficiency is 19% as compared to 19.7% reported by Bombarda et al. (2012).

3.1. Effect of mass fraction of hydrochloric acid

It is very important to study the effect of mass fraction of hydrochloric acid as it is a factor which determines the amount of hydrogen and oxygen which will be produced by the cycle. The effect of variation in mass fraction of hydrochloric acid at state 11 on the rate of hydrogen and oxygen production is shown in Fig. 3. It is observed that the rate of hydrogen production decreases gradually whereas the rate of oxygen production increases, respectively with increase in the mass fraction of hydrochloric acid at state 11. The rate of hydrogen production by Cu–Cl cycle, external electrolyzer and integrated system vary from 8.85 L/s to 4.81 L/s, 0.8969 L/s to 0.8921, and 9.8 L/s to 5.7 L/s, respectively with increase in mass fraction of hydrochloric acid at state 11 from 0.75 to 0.84. The rate of oxygen production is found to be increasing from 0.82 L/s to 1.08 L/s with increase in mass fraction of HCl at state 11. This behavior is noticed because increase in mass fraction of HCl results in a lesser amount of water in the solution entering the electrolyzer. As the amount of water entering the electrolyzer decreases the rate of hydrogen production also decreases. On the other hand, this increase in mass fraction of HCl results in higher amount of Cu_2OCl_2 production in S1 and therefore increasing the rate of oxygen production in S2. It is also important to notice that maintaining enough amount of water in the HCl solution is very important as concentrated HCl is very harmful and can damage the equipments.

Fig. 4 illustrates the effect of increase in mass fraction of HCl at state 11 on the energy efficiencies. The energy efficiency of the system without heat recovery, with heat recovery and with integration is found to be varying from 48.76% to 46.91%, 55.86% to 53.21% and 59% to 59.4%, respectively. This behavior is observed due to the fact that in without heat recovery system all the heat rejected by the system is dumped into the atmosphere

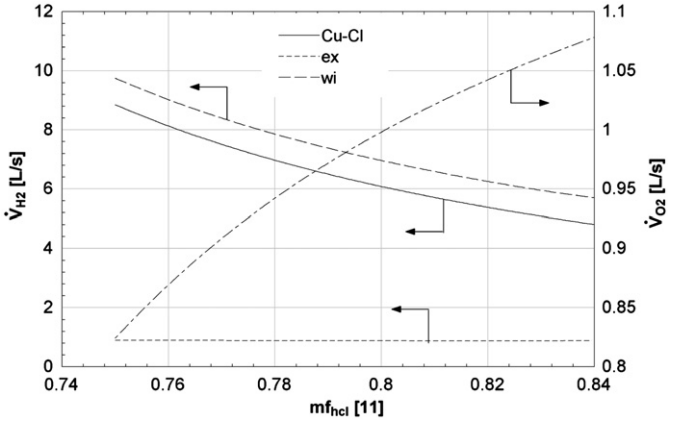

Fig. 3. Effect of mass fraction of hydrochloric acid at state 11 on rate of hydrogen productions of the Cu–Cl cycle only, external electrolyzer only and integrated system and rate of oxygen production for the Cu–Cl cycle.

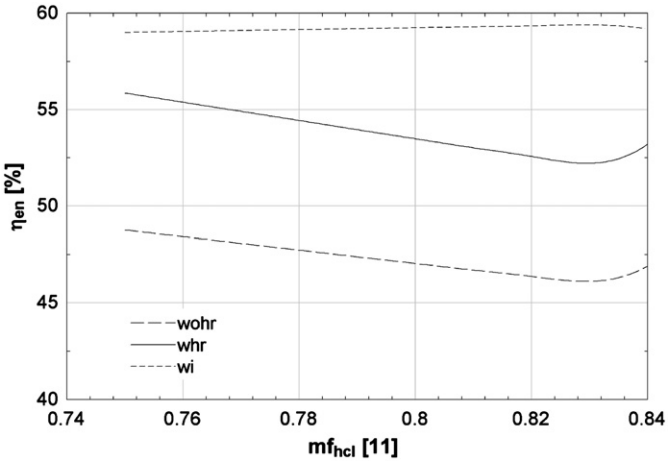

Fig. 4. Effect of mass fraction of hydrochloric acid at state 11 on energy efficiencies.

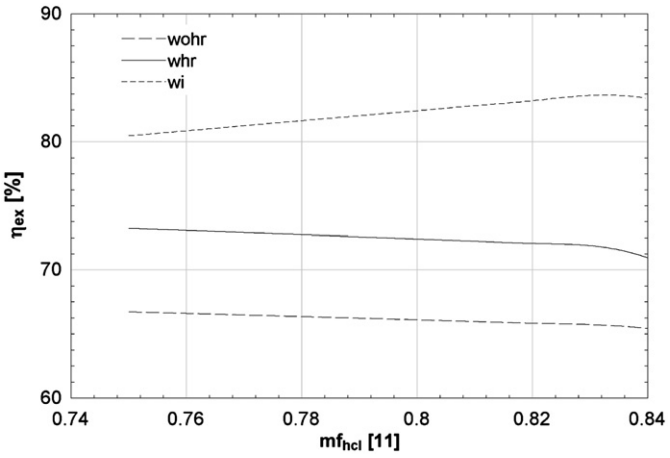

Fig. 5. Effect of mass fraction of hydrochloric acid at state 11 on exergy efficiencies.

whereas in heat recovery system all of the waste heat is recycled backed and is utilized to enhance the efficiency. Moreover, in integrated system the heat carried by the stream after passing through the heat recovery loop is supplied to an external system in order to produce extra output which further enhances the performance of the system. Also, the minimum one is observed at 0.83 due to increase in energy required by the cycle after a certain mass fraction value. The effect of increase in mass fraction of HCl at state 11 on the exergy efficiencies is shown in Fig. 5. It can be observed that the exergy efficiency of the system without heat recovery, with heat recovery, and with integration vary from 66.73% to 65.44%, 72.0% to 70.52%, and 78.28% to 81.29%, respectively. It is observed, that increase in mass fraction results in lower energy efficiency of the Cu–Cl cycle. Such behavior is observed because from energy perspective the rate of hydrogen production decreases with increase in mass fraction. However, exergy efficiencies help us see that the exergy efficiencies of the without heat recovery system and with heat recovery system decreases but exergy efficiency of the integrated system increases with increase in mass fraction. This behavior is noticed because although the rate of hydrogen production decreases with increase in mass fraction but the rate of oxygen production increases. The rate of oxygen production is taken as a useful output and therefore it helps improve the performance of the system and hence increases the efficiency of the system.

3.2. Effect of electrolyzer pressure

Studies conducted by researchers have shown that running the electrolyzer at high pressure has many positive attributes toward the hydrogen production as it generates compressed hydrogen which can be readily supplied to the end user (Zamfirescu et al. 2012). It can be seen in Fig. 6 that energy efficiencies increase with increase in electrolyzer pressure. The energy efficiency of the system without heat recovery, with heat recovery, and with integration is found to be varying from 47.02% to 51.86%, 53.47% to 64.39% and 59.22% to 63.93%, respectively with increase in electrolyzer pressure from 100 kPa to 1000 kPa. The exergy efficiency of the system without heat recovery, with heat recovery, and with integration is found to be varying from 66.06% to 73.78%, 71.0% to 87.24% and 80.23% to 90.4%, respectively with increase in electrolyzer pressure as shown in Fig. 7. Table 1 This kind of behavior is noticed because of the fact that an increase in pressure results in a higher energy content of the hydrogen and oxygen due to the decrease in energy requirement by the electrolyzer for hydrogen production. Also, increase in pressure makes water molecules more unstable which makes it easy to dissociate the water bond and hence reduce the energy requirement of the electrolyzer. It is also noticed that until the pressure reaches 400 kPa, the present integrated system has the best efficiency but after 400 kPa system with heat recovery shows slightly better performance. Moreover, for the without heat recovery system and with heat recovery system a local maximum

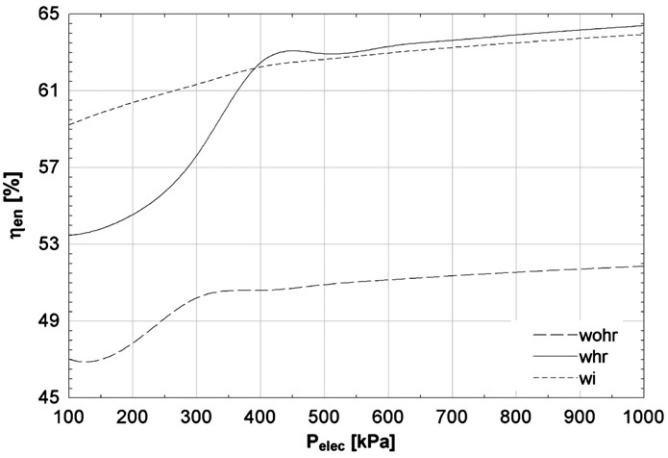

Fig. 6. Effect of electrolyzer pressure on energy efficiencies.

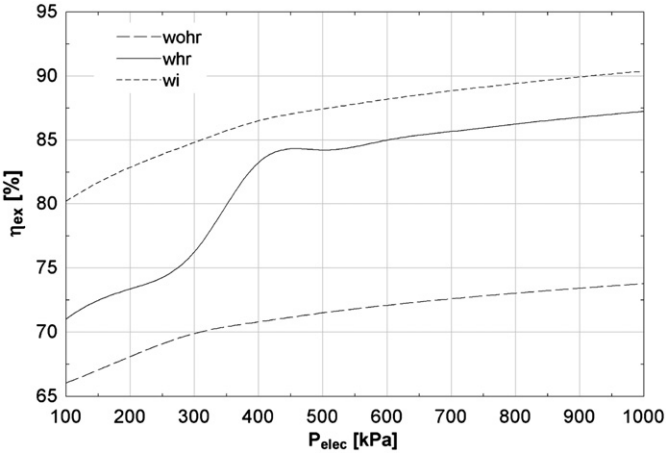

Fig. 7. Effect of electrolyzer pressure on exergy efficiencies.

Table 1
Thermodynamic properties of Cu–Cl cycle.

State number	Pressure (kPa)	Temperature (K)	Mass flow rate (kg/s)	Specific enthalpy (kJ/kg)	Specific entropy (kJ/kg K)
1	101.3	298.2	0.001802	104.8	0.3669
2	23.08	298.2	0.003156	104.8	0.3669
3	101.3	298.2	0.003156	104.9	0.367
4	101.3	298.2	0.004957	104.9	0.367
5	101.3	342.2	0.004957	288.9	0.9427
6	101.3	486.2	0.004957	2900	7.881
7	101.3	581.2	0.004957	3090	8.237
8	101.3	673.2	0.004957	3278	8.537
9	101.3	673.2	0.07156	2336	4.069
10	101.3	673.2	0.05578	3316	3.429
11	101.3	673.2	0.01578	−1128	6.507
12	101.3	385.2	0.01578	−1428	5.926
13	101.3	373.2	0.01578	−1441	5.894
14	101.3	298.2	0.01578	−2004	4.249
15	101.3	298.2	0.01578	−2004	4.249
16	101.3	755.2	0.05578	3352	3.48
17	101.3	773.2	0.05578	3360	3.49
18	101.3	773.2	0.05578	3521	3.277
19	6.977	773.2	0.001302	467.6	8.03
20	94.35	773.2	0.05448	3594	3.189
21	6.977	690.2	0.001302	381.6	7.913
22	6.977	585.2	0.001302	275	7.745
23	94.35	298.2	0.01262	−2493	5.142
24	94.35	696.2	0.05448	3564	3.147
25	94.35	682.2	0.05448	3558	3.139
26	94.35	298.2	0.05448	3408	2.816
27	101.3	298.2	0.01628	−1822	5.968
28	45.61	298.2	0.01262	−2532	5.308
29	32.63	298.2	0.0004993	3931	58.05
31	101.3	298.2	0.06859	2440	2.823
32	101.3	323.2	0.06859	2453	2.865
33	101.3	353.2	0.06859	2535	3.113
34	18.42	353.2	0.001983	2648	8.057
35	18.42	298.2	0.001983	104.8	0.3669
36	94.35	298.2	0.001983	104.8	0.3669
37	101.3	353.2	0.06661	2532	2.966
38	101.3	651.2	0.06661	2658	3.224
39	101.3	673.2	0.06661	2667	3.238
41	94.35	298.2	0.06909	266	2.844
42	94.35	298.2	0.06909	266	2.844
43	101.3	298.2	0.06909	266	2.836

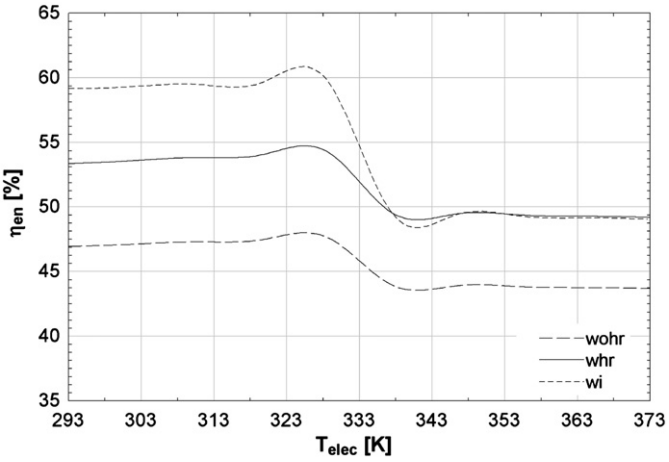

Fig. 8. Effect of electrolyzer temperature on energy efficiencies.

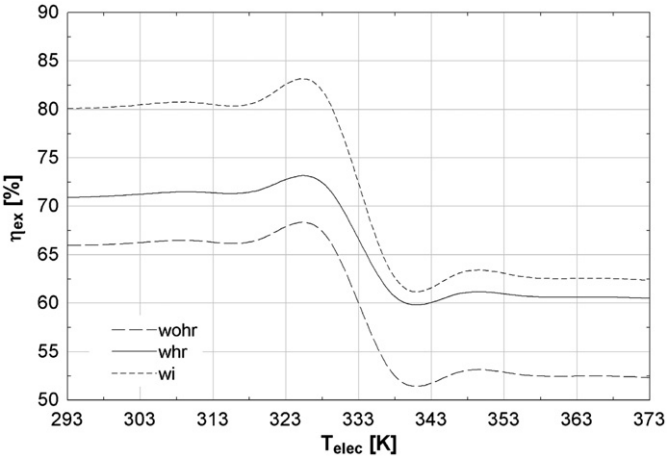

Fig. 9. Effect of electrolyzer temperature on exergy efficiencies.

appears due to sudden decrease in energy requirement of the cycle. The energy content of any solution is dependent on its thermophysical properties, such as pressure and the energy content of a solution, and changes suddenly when the thermophysical properties cross certain limits such as going from saturated mixture to saturated vapor form.

3.3. Effect of electrolyzer temperature

The electrolyzer temperature determines the amount of energy carried by the hydrogen and other products leaving the electrolyzer. Fig. 8 shows the effect of electrolyzer temperature on the energy efficiencies. The energy efficiency of the system without heat recovery, with heat recovery, and with integration is found to be varying from 46.94% to 43.68%, 53.35% to 49.19% and 59.15% to 49.02%, respectively with increase in electrolyzer temperature from 293 K to 373 K. The exergy efficiency of the system without heat recovery, with heat recovery, and with integration is found to be varying from 65.97% to 52.31%, 70.91% to 60.49%, and 80.11% to 62.37%, respectively as shown in Fig. 9. It is observed in Figs. 8 and 9 that there is a point at which maximum efficiencies are obtained and after this point the efficiencies start decreasing again. Such behavior is noticed, because energy content of any solution is dependent on its thermophysical properties (such as temperature and pressure) and once a certain limit of these thermophysical quantities is crossed then either increase or decrease in energy content of the solution is observed. The analyses show that it is best to operate electrolyzer at 328.6 K because at this temperature maximum energy and exergy efficiencies are obtained. The maximum energy efficiency of the system without heat recovery, with heat recovery, and with integration obtained is 47.66%, 54.29%, and 59.81%, respectively. The maximum exergy efficiency of the system without heat recovery, with heat recovery, and with integration obtained is 66.92%, 72.06%, and 81.32%, respectively.

3.4. Effect of ambient temperature

Ambient temperature plays an important role in performance determination of many systems such as thermochemical water splitting cycles. Fig. 10 illustrates the effect of rise in ambient temperature on rate of hydrogen and oxygen production. It can be seen that rate of hydrogen produced by the Cu–Cl cycle, external electrolyzer and integrated system vary from 5.57 L/s to 6.6 L/s, 0.81 L/s to 0.95 L/s and 6.38 L/s to 7.6 L/s, respectively with rise in ambient temperature from 273 K to 323 K. The oxygen production rate is found to be varying from 0.91 L/s to 1.1 L/s with rise in ambient temperature. This behavior is observed because thermochemical cycles are mostly driven by temperatures. The change in ambient temperature results in fluctuation in heat loss to the

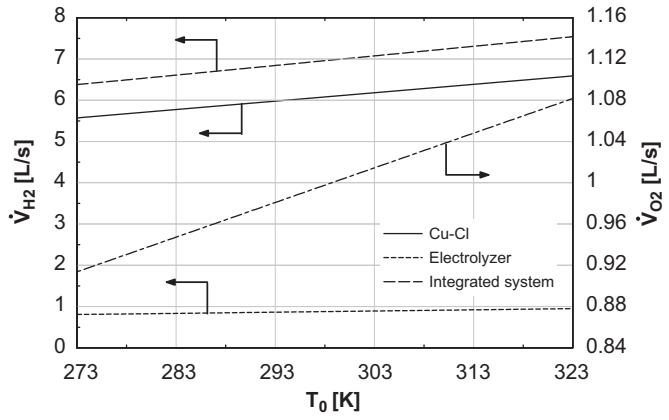

Fig. 10. Effect of ambient temperature on rate of hydrogen productions of the Cu–Cl cycle only, external electrolyzer only and the integrated system and rate of oxygen production of the Cu–Cl cycle.

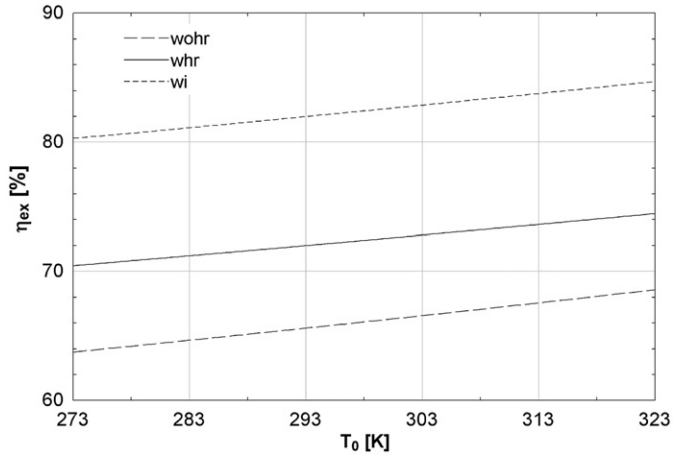

Fig. 11. Effect of ambient temperature on exergy efficiencies.

environment and therefore resulting in fluctuating performance of the system. Fig. 11 helps us see the effect of rise in ambient temperature on the exergy efficiencies. The exergy efficiency of the system without heat recovery, with heat recovery, and with integration is observed to be varying from 63.75% to 68.59%, 68.97% to 73.26%, and 77.81% to 82.91%, respectively with rise in ambient temperature. The increasing trend of exergy efficiencies with rise in ambient temperature is observed because rise in temperature results in lesser amount of heat being lost due to the temperature difference between the system and environment therefore, enhancing the performance of the system.

3.5. Exergy destruction rate

Fig. 12 illustrates the exergy destruction rate in each component of the integrated system. This figure helps locating the subsystem which hampers the performance of the system the most. It can be seen that in Cu–Cl cycle maximum amount of exergy is destructed in the S1 (16.82 kW) and in the Kalina cycle maximum amount of exergy is destructed in heat exchanger (48.05 kW) where heat is transferred from weak solution to the strong solution entering the generator. This shows that in order to enhance the performance of the Cu–Cl cycle, efforts should be made to reduce the exergy destruction rate occurring in S1. In the

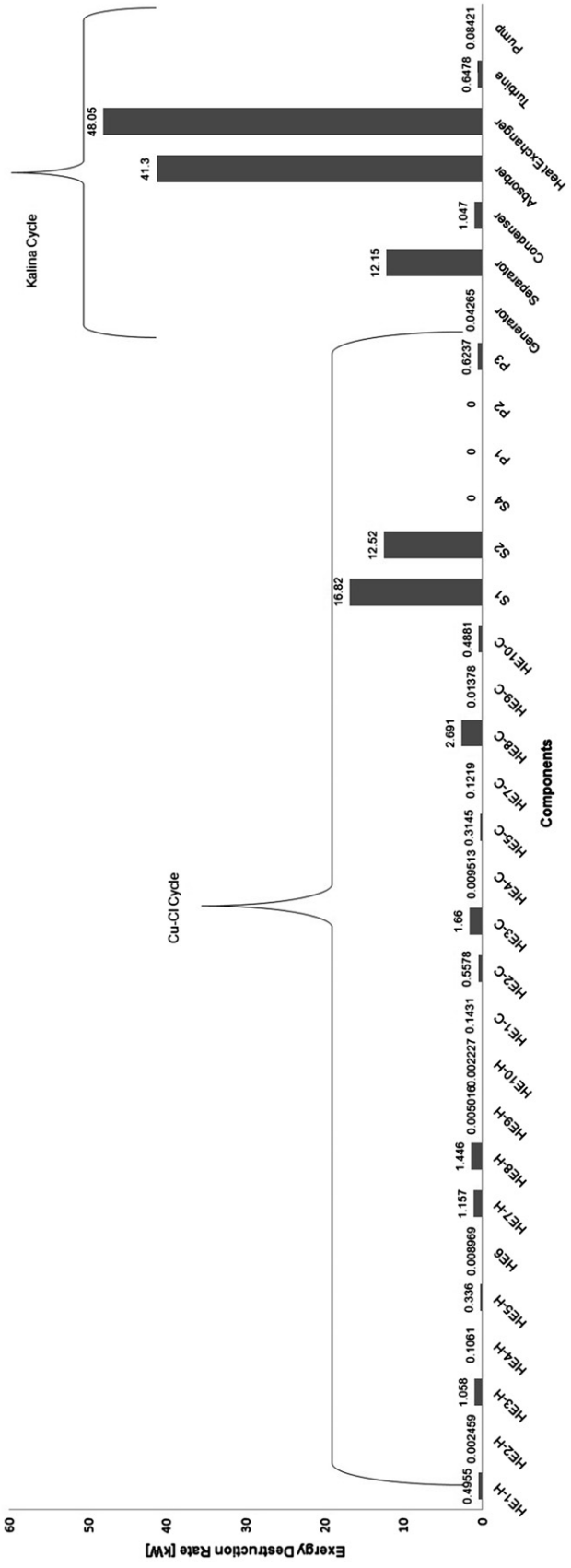

Fig. 12. Exergy destruction rate in each component of the integrated system.

Kalina cycle special attention should be given to the heat exchanger in order to enhance the performance of the Kalina cycle.

4. Conclusions

This paper focuses on energy and exergy analyses of an integrated Cu–Cl thermochemical cycle and Kalina cycle system for hydrogen production. A parametric study is conducted to investigate the effects of several operating parameters such as mass fraction of hydrochloric acid, electrolyzer pressure, electrolyzer temperature and ambient temperature on the rate of hydrogen produced, rate of oxygen produced and energy and exergy efficiencies of the system. A comparative assessment is carried out to study the effect of operating parameters on the efficiencies of three Cu–Cl cycle cases namely system without heat recovery, system with heat recovery and integrated system. In the exergy destruction bar chart is presented for a base case to show which component in the cycle destructs most amount of exergy. The results obtained show that rate of hydrogen produced decreases with increase in mass fraction of HCl whereas, rate of oxygen produced increases with increase in mass fraction of HCl. It is also observed that energy and exergy efficiencies decrease with increase in mass fraction of HCl. The pressure analysis show that energy and exergy efficiencies increase with increase in pressure of the electrolyzer. It is also observed that an optimum operating temperature is 328.6 K because at this temperature, energy and exergy efficiencies become 66.92% and 72.06%, respectively. The ambient temperature analysis revealed that the exergy efficiencies increase with rise in ambient temperature. After looking at exergy destruction chart it is concluded that in the Cu–Cl cycle the highest amount of exergy is destructed by S1 (16.82 kW) and in the Kalina cycle the highest amount of exergy is destructed by heat exchanger (48.05 kW). The limitation for the integration of this kind of the Kalina cycle may come down to the equipment required for the Kalina cycle as they require different types of turbines and/or expanders at such a large scale.

Nomenclature

$\dot{E}x$	exergy destruction rate, kW
h	specific enthalpy, kJ/kg
HHV	higher heating value
m	mass flow rate, kg/s
M	molecular weight, kg/mol
mf	mass fraction
nw	water for heat recovery
P	pressure, kPa
$\dot{Q}$	heat flow rate, kW
T	temperature, K
s	specific entropy, kJ/kg K
S	separator
$\dot{W}$	work rate, kW
y	mole fraction

Greek letters

η	efficiency

Subscripts

ch	chemical
conv	conversion
elec	electrolyzer
en	energy
ex	exergy
H_2	hydrogen
i	*i*th state
iso	isobutane
k	*k*th state
m	*m*th state
p	pump
ph	physical
th	thermal
turb	turbine
whr	with heat recovery
wi	with integrations
wohr	without heat recovery

Acronyms

C	cold
HE	heat exchanger
H	hot
S	separator
SEP	separator
SMR	steam methane reforming

References

Aghahosseini, S., Dincer, I., Naterer, G., 2011. Integrated gasification and Cu–Cl cycle for trigeneration of hydrogen, steam and electricity. Int. J. Hydrogen Energy 36, 2845–2854.

Bombarda, P., Invernizzi, C.M., Pietra, C., 2012. Heat recovery from diesel engines: a thermodynamic comparison between Kalina and ORC cycles. Appl. Therm. Eng. 30, 212–219.

Dincer, I., Rosen, M.A., 2007. Exergy; Energy Environment And Sustainable Development. Springer, Oxford.

Dufour, J., Serrano, D.P., Galvez, J.L., Moreno, J., Garcia, C., 2009. Life cycle assessment of processes for hydrogen production: environmental feasibility and reduction of greenhouse gases emissions. Int. J. Hydrogen Energy 34, 1370–1376.

Ferrandon, M.S., Lewis, M.A., Tatterson, D.F., Gross, A., et al., 2010. Hydrogen production by the Cu–Cl thermochemical cycle: investigation of the key step of hydrolysing $CuCl_2$ to Cu_2OCl_2 and HCl using a spray reactor. Int. J. Hydrogen Energy 35, 992–1000.

Giaconia, A., Sau, S., Felici, C., Tarquini, P., Karaginnakis, G., Pagkoura, C., et al., 2011. Hydrogen production via sulfur-based thermochemical cycles: Part 2: performance evaluation of Fe_2O_3-based catalysts for the sulfuric acid decomposition step. Int. J. Hydrogen Energy 36, 6496–6509.

Klein SA. 2012. Engineering Equation Solver (EES), Academic Commercial. F-Chart Software, Madison, WI. www.fChart.com.

Lewis, M.A., Masin, J.G., Vilim, R.B., 2010. Development of the low temperature Cu–Cl thermochemical cycle. Int. Cong. Adv. Nucl. Power Plants.

Midilli, A., Dincer, I., 2009. Development of some exergetic parameters for PEM fuel cells for measuring environmental impact and sustainability. Int. J. Hydrogen Energy 34, 3858–3872.

Midilli, A., Dincer, I., 2008. Hydrogen as a renewable and sustainable solution in reducing global fossil fuel consumption. Int. J. Hydrogen Energy 33, 4209–4222.

Moriarty, P., Honnery, D., 2009. Hydrogen's role in an uncertain energy future. Int. J. Hydrogen Energy 34, 31–39.

Muradov, N.Z., Veziroglu, T.N., 2008. "Green" path from fossil-based to hydrogen economy: an overview of carbon-neutral technologies. Int. J. Hydrogen Energy 33, 6804–6839.

Naterer, G.F., Suppiah, S., Stilberg, L., Lewis, M., et al., 2011a. Clean hydrogen production with the Cu–Cl cycle—progress of international consortium, II: simulations, thermochemical data and materials. Int. J. Hydrogen Energy 36, 15486–15501.

Naterer, G.F., Suppiah, S., Stilberg, L., Lewis, M., et al., 2011b. Clean hydrogen production with the Cu–Cl cycle–progress of international consortium, I: experimental unit operations. Int. J. Hydrogen Energy 36, 15472–15485.

Orhan, M.F., Dincer, I., Rosen, M.A., 2011. Design of systems for hydrogen production based on the Cu–Cl thermochemical water decomposition cycle: configurations and performance. Int. J. Hydrogen Energy 36, 11309–11320.

Orhan, M.F., Dincer, I., Rosen, M.A. Efficiency comparison of various design schemes for copper–chlorine (Cu–Cl) hydrogen production processes using

Aspen Plus software, Energy Convers. Manage., http://dx.doi.org/10.1016/j.enconman.2012.01.029, in press.
Ozbilen, A., Dincer, I., Rosen, M.A., 2011. Environmental evaluation of hydrogen production via thermochemical water splitting using the Cu–Cl cycle: a parametric study. Int. J. Hydrogen Energy 36, 9514–9528.
Turner, J.A., 2004. Sustainable hydrogen production. Science 305, 972–974.
Zamfirescu, C., Dincer, I., Naterer, G., 2010. Thermophysical properties of copper compounds in copper–chlorine thermochemical water splitting cycles. Int. J. Hydrogen Energy 35, 4839–4852.
Zamfirescu, C., Naterer, G., Dincer, I., 2012. Photo-electro-chemical chlorination of cuprous chloride with hydrochloric acid for hydrogen production. Int. J. Hydrogen Energy 37, 9529–9536.